Numerical Analysis of Schrödinger Equation for a Magnetized Particle in the Presence of a Field Particle*)

Shun-ichi OIKAWA, Emi OKUBO[1)] and Poh Kam CHAN[1)]

Faculty of Engineering, Hokkaido University, Sapporo 060-8628, Japan

[1)]*Graduate School of Engineering, Hokkaido University, Sapporo 060-8628, Japan*

(Received 9 December 2011 / Accepted 22 May 2012)

We have solved the two-dimensional time-dependent Schödinger equation for a magnetized proton in the presence of a fixed field particle with an electric charge of $2\times10^{-5}e$, where e is the elementary electric charge, and of a uniform megnetic field of $B = 10$ T. In the relatively high-speed case of $v_0 = 100$ m/s, behaviors are similar to those of classical ones. However, in the low-speed case of $v_0 = 30$ m/s, the magnitudes both in momentum $mv = |m\boldsymbol{v}|$, where m is the mass and $\boldsymbol{v}$ is the velocity of the particle, and position $r = |\boldsymbol{r}|$ are appreciably decreasing with time. However, the kinetic energy $K = m\langle\boldsymbol{v}^2\rangle/2$ and the potential energy $U = \langle qV\rangle$, where q is the electric charge of the particle and V is the scalar potential, do not show appreciable changes. This is because of the increasing variances, i.e. uncertainty, both in momentum and position. The increment in variance of momentum corresponds to the decrement in the magnitude of momentum: Part of energy is transfered from the directional (the kinetic) energy to the uncertainty (the zero-point) energy.

Keywords: uncertainty, field particle, uniform magnetic field, magnetic length, quantum mechanical effect

DOI: 10.1585/pfr.7.2401106

1. Introduction

We have shown in the previous paper [1] that the variance, or the uncertainty, in position would reach the square of the interparticle separation $n^{-2/3}$ with a number density of $n = 10^{20}\,\mathrm{m}^{-3}$ in a time interval of the order of 10^{-4} sec. After this time the wavefunctions of neighboring particles would overlap, as a result the conventional classical analysis may lose its validity: Plasmas may behave more-or-less like extremely-low-density liquids, not gases, since the size of each particle is of the same order of the interparticle separation.

We have also pointed out [2–4] that (i) for distant encounters in typical fusion plasmas of a temperature $T = 10\,\mathrm{keV}$ and $n = 10^{20}\,\mathrm{m}^{-3}$, the average potential energy $\langle U\rangle \sim 30\,\mathrm{meV}$ is as small as the uncertainty in energy $\Delta E \sim 40\,\mathrm{meV}$, and (ii) for a magnetic field $B \sim 3\,\mathrm{T}$, the spatial size of the wavefunction in the plane perpendicular to the magnetic field is as large as the magnetic length $\ell_\mathrm{B} \sim 10^{-8}$ m [5] which is much larger than the typical electron wavelength $\lambda_\mathrm{e} \sim 10^{-11}$ m, and is around one-tenth of the average interparticle separation $\Delta\ell$.

In considering the diffusion of plasmas correctly, it was pointed out more than half a century ago [6, 7] that one must consider the wave character of charged particles when the temperature T is high, i.e. the relative speeds of interacting particles are fast. The criterion on the classical theory to be valid in terms of relative speed g in a hydrogen plasma is given in Ref. [7], as

$$g \ll \frac{2e^2}{4\pi\epsilon_0\hbar} = 4.4\times10^6\ \mathrm{m/s}, \tag{1}$$

where $e = 1.60\times10^{-19}$ C and $\hbar \equiv h/2\pi = 1.05\times10^{-34}$ J·s stand for the elementary electric charge and the reduced Planck constant. In contemporary fusion plasmas with $T \sim 10$ keV or higher, ions as well as electrons should be treated quantum mechanically. In current plasma physics, however, the quantum mechanical effects enters as a minor correction to the Coulomb logarithm in the case of close encounters [8]. Nonetheless, the neoclassical theory [9] is capable of predicting a lot of phenomena such as those related to the current conduction. In this paper, as an extention of previous study of Ref. [2], quantum mechanical effects of a field particle in the presence of a uniform magnetic field will be studied.

2. Schrödinger Equation

The unsteady Schrödinger equation for wavefunction $\psi(\boldsymbol{r}, t)$, at a position $\boldsymbol{r}$ and a time t, is given by

$$\mathrm{i}\hbar\frac{\partial\psi}{\partial t} = \left[\frac{1}{2m}\left(-\mathrm{i}\hbar\nabla - q\boldsymbol{A}\right)^2 + qV\right]\psi, \tag{2}$$

where $V = V(\boldsymbol{r})$ and $\boldsymbol{A} = \boldsymbol{A}(\boldsymbol{r})$ stand for the scalar and vector potentials, m and q the mass and electric charge of the particle under consideration, and $\mathrm{i} \equiv \sqrt{-1}$ the imaginary unit. When the corresponding classical particle has a momentum $\boldsymbol{p}_0 = m\boldsymbol{v}_0$, where $\boldsymbol{v}_0$ is the initial velocity, at a

author's e-mail: e-okubo@fusion.qe.eng.hokudai.ac.jp

*) This article is based on the presentation at the 21st International Toki Conference (ITC21).

position $\boldsymbol{r} = \boldsymbol{r}_0$ at a time $t = 0$, the initial condition for the wavefunction $\psi(\boldsymbol{r}, 0)$ can be given [10, 11] by

$$\psi(\boldsymbol{r}, 0) = \frac{1}{\sqrt{\pi}\ell_{\mathrm{B}}} \exp\left[-\frac{(\boldsymbol{r} - \boldsymbol{r}_0)^2}{2\ell_{\mathrm{B}}^2} + \mathrm{i}\boldsymbol{k}_0 \cdot \boldsymbol{r}\right], \tag{3}$$

where $\boldsymbol{k}_0 = m\boldsymbol{v}_0/\hbar$ is the initial wavenumber vector.

We will solve Eqs. (2) and (3) using the finite difference method (FDM) in space with the Crank-Nicolson scheme [1, 11, 12].

We will adopt the successive over relaxation (SOR) scheme for time integration.The size of spatial discretization for the *two-dimensional* FDM in (x, y) plane should be sufficiently small to satisfy

$$\Delta x \sim \Delta y \ll \frac{1}{k_0} = \frac{\lambda_0}{2\pi}, \tag{4}$$

where λ_0 is the de Broglie wavelength. This restriction Eq. (4) on Δx and Δy demands a lot of computer memory for fast particles.

2.1 Electrostatic potential due to a field particle

Here we have assumed that the field particle is a quantum-mechanical particle centered at the origin with the wavefunction ψ_{f} similar to that given in Eq. (3), but is fixed in space and time, as

$$\psi_{\mathrm{f}}(\boldsymbol{r}) = \frac{\exp\left(-\frac{x^2+y^2}{2\ell_{\mathrm{B}}^2}\right)}{\sqrt{\pi\ell_{\mathrm{B}}^2}} \times \frac{\exp\left(-\frac{z^2}{2\sigma_z^2}\right)}{\sqrt{\pi^{1/2}\sigma_z}}, \tag{5}$$

where σ_z^2 is the variance in position in z-direction. In magnetically confined fusion plasmas, $\sigma_z \sim h/mv_0 \ll \ell_{\mathrm{B}}$ holds, so that the square of the second factor can be approximately the same as a Dirac delta function $\delta(z)$ centered at $z = 0$. Thus the electrostatic potential φ_{f} in the x-y plane, due to the distributed charge is given by

$$\varphi_{\mathrm{f}}(R) \simeq \frac{q_{\mathrm{f}}}{4\pi\epsilon_0\ell_{\mathrm{B}}^2}\frac{4}{\pi}\int_0^\infty \frac{R'\mathrm{e}^{-(R'/\ell_{\mathrm{B}})^2}}{R + R'} K(M)\,\mathrm{d}R', \tag{6}$$

where $R = \sqrt{x^2 + y^2}$, q_{f} is an electric charge of the field particle, ϵ_0 is the vacuum permittivity, and $K(M)$ is the complete elliptic integral of the first kind with the parameter M being defined as $M \equiv 4RR'/(R + R')^2$ [13].

3. Numerical Results

In what follows, velocity and time are normalized by 10 m/s and the cyclotron frequency for a proton in $B = 10$ T with a speed of 10 m/s, thus position is normalized by the cyclotron radius of the proton. The magnetic length [5] for a proton in $B = 10$ T, $\ell_{\mathrm{B}} \equiv \sqrt{\hbar/eB} \sim 10^{-8}$ m is a measure for the spread of a wave function in the plane perpendicular to the magnetic field. With these normalization, Planck constant $\hbar \sim 0.60$, initial uncertainty in position $\ell_{\mathrm{B}}^2 = \hbar/eB \sim 0.78^2$ and initial uncertainty in kinetic momentum $\frac{3}{2}\hbar eB \sim 0.91$ are of order of unity. It should be noted that the kinetic energy of a classical proton speed ~ 27 m/s in $B = 10$ T corresponds to the uncertainty of the momentum. In the numerical results to be presented in the following subsections, the Schrödinger equation is solved for a time duration of five cyclotron rotations by a proton.

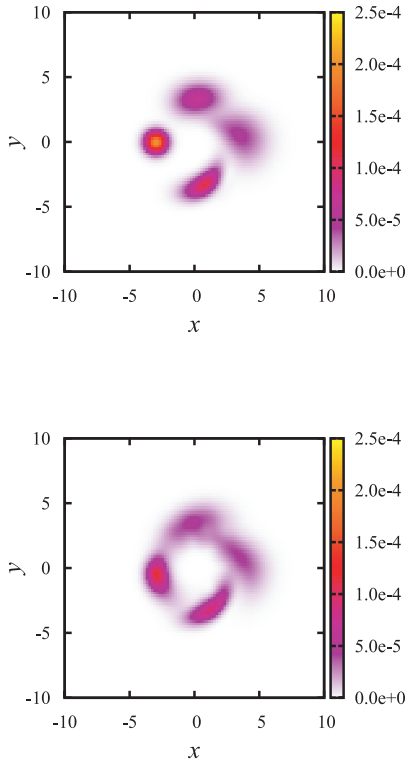

Fig. 1 Time evolution of probability density function (PDF) for $v_0 = 30$ m/s, $B = 10$ T, and $q_{\mathrm{f}} = 2 \times 10^{-5}e$. The PDFs for the first cyclotron rotation are depicted on the top, in which the initial PDF is the smallest circle in shape centered at $(x_0, y_0) = (-3, 0)$. PDF rotate clockwise with time. The figure on the bottom is for the second rotation.

Figure 1 shows the time evolution of probability density function (PDF) for $v_0 = 30$ m/s, $B = 10$ T, and $q_{\mathrm{f}} = 2 \times 10^{-5}e$, where e is the elementary electric charge. The PDFs at four different times, $\omega t = 0, \pi/2, \pi, 3\pi/2$, where ω is the cyclotron angular frequency, for the first cyclotron rotation are depicted on the top, in which the initial PDF is the smallest circle in shape centered at $(x_0, y_0) = (-3, 0)$. PDF rotates clockwise with time. The figure on the bottom is for the second rotation. It is seen that the PDF changes from a circular shape to elongated one along the direction the particle moves.

3.1 Errors in energy and particle conservation

The numerical errors in energy and particle conservation for the field particle charge of $q_{\mathrm{f}} = 2 \times 10^{-5}e$ is quite small, as shown in Fig. 2 for initial speed of $v_0 = 100$ m/s, and Fig. 3 for $v_0 = 30$ m/s. The time evolution of energies, the kinetic energy $K = m\langle \boldsymbol{v}^2 \rangle/2$ and the potential energy $U = \langle qV \rangle$, for $v_0 = 30$ m/s is shown in Fig. 4. Note

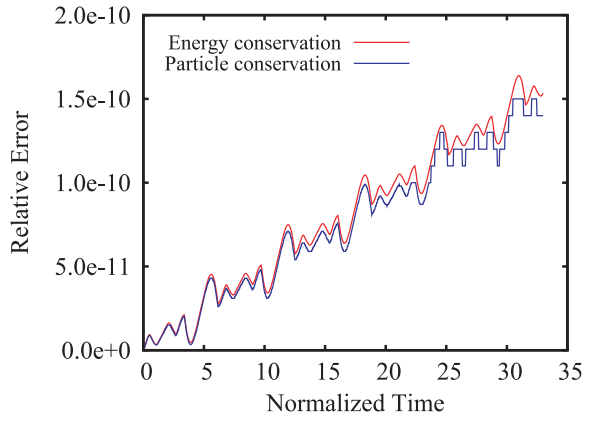

Fig. 2 Time evolution of relative errors in energy and particle conservation for $B = 10$ T and $q_f = 2 \times 10^{-5}e$. Initial speed is $v_0 = 100$ m/s.

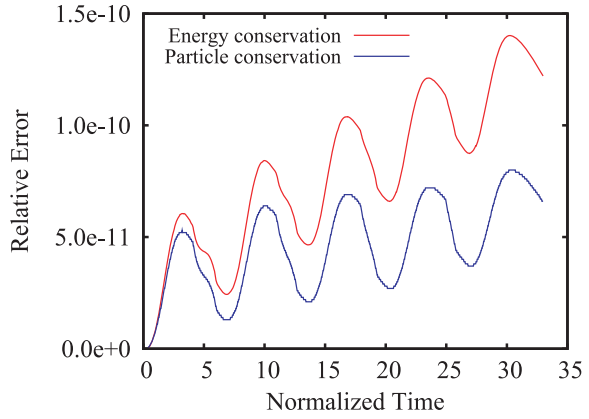

Fig. 3 Time evolution of relative errors in energy and particle conservation for $B = 10$ T and $q_f = 2 \times 10^{-5}e$. Initial speed is $v_0 = 30$ m/s.

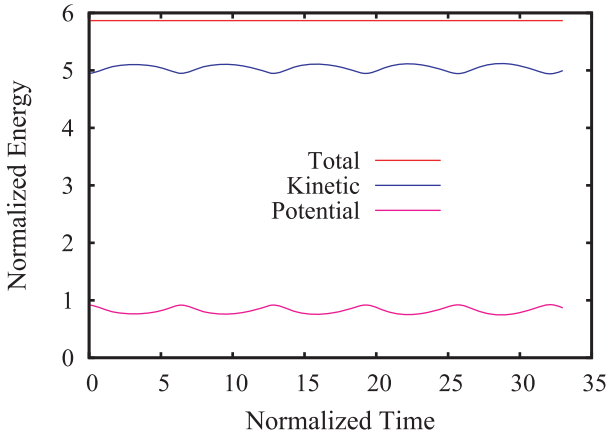

Fig. 4 Time evolution of normalized energies; kinetic K, potential U, and total $E = K + U$ for $v_0 = 30$ m/s, $B = 10$ T, and $q_f = 2 \times 10^{-5}e$.

that the electric charge q_f of the field particle is intentionally assumed small, since $q_f = e$ with $v_0 = 30$ - 100 m/s makes the potential energy much larger than that of kinetic energy. Such a situation seldom occur in low density and high temperature plasmas. The initial speed $v_0 = 30$ - 100 m/s, which is much slower than a thermal speed of fusion plasmas, is assumed here due to a numerical reason: required numerical grid sizes Δx and Δy in Eq. (4) need to be much smaller than the de Broglie wavelength that is inversely proportional to the particle speed. The combination $v_0 = 30$ - 100 m/s and $q_f \sim 10^{-10}e$ leads to the similar potential to kinetic energy ratio as found in fusion plasmas.

3.2 Expectation values and variaces

Depicted lines in blue on the left and in the center in Fig. 5 are expectation values $\langle m\boldsymbol{v}\rangle$ and $\langle \boldsymbol{r}\rangle$ for $v_0 = 100$ m/s, respectively, in which the classical counterparts are also plotted in red. On the right in Fig. 5 shows the time evolution of normalized variances of momentum $\sigma_p^2 = \langle (m\boldsymbol{v})^2\rangle - \langle m\boldsymbol{v}\rangle^2$ in blue, and position $\sigma_r^2 = \langle \boldsymbol{r}^2\rangle - \langle \boldsymbol{r}\rangle^2$ in red. The trajectory in the phase space $(\boldsymbol{r}, \boldsymbol{p})$ is close to the classical one, and variances show simple oscillation with almost constant amplitudes.

Similar plots for $v_0 = 30$ m/s are shown in Fig. 6. Both trajectories in the momentum space and the configuration space are gradually decreasing in radii with time, which is opposed to the classical trajectory as shown in these figures with red lines. In addition, variances both in momentum and configuration space grow with time.

The increment in variance of kinetic momentum, $\Delta\sigma_p^2 = \langle (m\boldsymbol{v})^2\rangle - \langle m\boldsymbol{v}\rangle^2 - \frac{3}{2}\hbar qB$, corresponds to the decrement in the magnitude of momentum as was shown in Fig. 4: Part of energy is transfered from the directional, or the kinetic, energy to the uncertainty, or the zero-point, energy. This is a result of energy conservation as shown in Fig. 3.

Thus, in the relatively high-speed case of $v_0 = 100$ m/s, behaviors are similar to those of classical ones. In the low-speed case of $v_0 = 30$ m/s, however, the magnitudes both in momentum $mv = |m\boldsymbol{v}|$ and position $r = |\boldsymbol{r}|$ are appreciably decreasing with time, as shown on the left in Figs. 5 and 6. The kinetic energy $K = m\langle \boldsymbol{v}^2\rangle/2$ and the potential energy $U = \langle qV\rangle$, however, do not show appreciable changes except for a small amplitude oscillation as shown in Fig. 4, because of the increasing variances, i.e. uncertainty, both in momentum and position.

4. Summary

We have solved the two-dimensional time-dependent Schödinger equation for a magnetized proton in the presence of a fixed field particle with an electric charge of $2 \times 10^{-5}e$ and of a uniform megnetic field of $B = 10$ T. In the relatively high-speed case of $v_0 = 100$ m/s, behaviors are similar to those of classical ones. In the low-speed case of $v_0 = 30$ m/s, however, the magnitudes both in momentum $mv = |m\boldsymbol{v}|$ and position $r = |\boldsymbol{r}|$ are appreciably decreasing with time. The kinetic energy $K = m\langle \boldsymbol{v}^2\rangle/2$ and the potential energy $U = \langle qV\rangle$, however, do not show

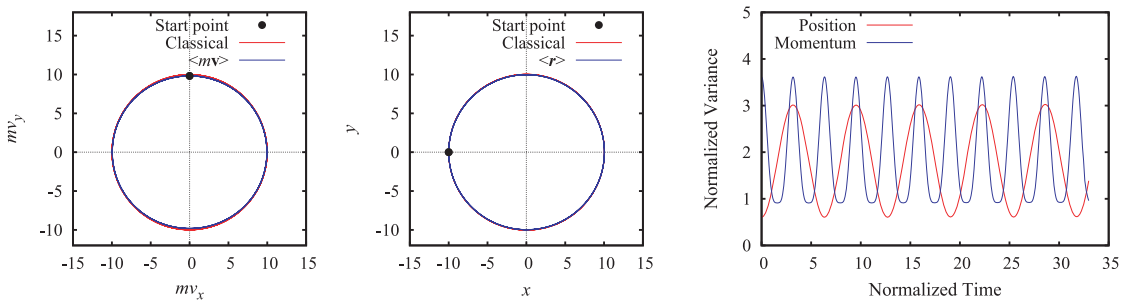

Fig. 5 Normalized expectation values of momentum $\boldsymbol{p} = \langle m\boldsymbol{v} \rangle$ in blue with classical one in red on the left, and of position $\langle \boldsymbol{r} \rangle$ in blue with classical one in red in the center. Depicted on the right are time evolution of normalized variances in mv-momentum $\sigma_{\rm p}^2 = \langle (m\boldsymbol{v})^2 \rangle - \langle m\boldsymbol{v} \rangle^2$ in blue and in position $\sigma_r^2 = \langle \boldsymbol{r}^2 \rangle - \langle \boldsymbol{r} \rangle^2$ in red, both for $B = 10$ T and $q_{\rm f} = 2 \times 10^{-5} e$. Initial particle speed is $v_0 = 100$ m/s.

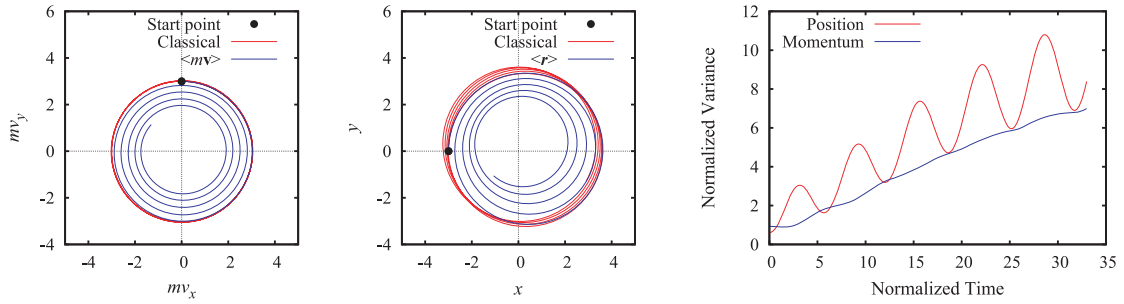

Fig. 6 Similar plots as Fig. 5 for initial particle speed $v_0 = 30$ m/s.

appreciable changes except for a small amplitude oscillation, because of the increasing variances, i.e. uncertainty, both in momentum and position.

The increment in variance of momentum corresponds to the decrement in the magnitude of momentum: Part of energy is transfered from the directional (the kinetic) energy to the uncertainty (the zero-point) energy.

In summary, quantum-mechanical analyses are necessary for slow particles with mass m and charge q in the presence of magnetic field B, whose kinetic energy K is of the order of $\hbar qB/2\,m$.

Acknowledgment

The authors would like to thank Prof. Y. Matsumoto and Prof. M. Itagaki for their fruitful discussions on the subject. Part of the SOR coding for a GPU was done by Mr. R. Ueda. This research was partially supported by a Grant-in-Aid for Scientific Research (C), 21560061.

[1] S. Oikawa, T. Shimazaki and E. Okubo, Plasma Fusion Res. **6**, 2401058 (2011).
[2] S. Oikawa, T. Oiwa and T. Shimazaki, Plasma Fusion Res. **5**, S1050 (2010).
[3] S. Oikawa, T. Oiwa and T. Shimazaki, Plasma Fusion Res. **5**, S2024 (2010).
[4] S. Oikawa, T. Shimazaki and T. Oiwa, Plasma Fusion Res. **5**, S2025 (2010).
[5] L.D. Landau and E.M. Lifshitz, *Quantum Mechanics*: *Non-relativistic Theory*, 3rd ed., translated from the Russian by J.B. Sykes and J.S. Bell (Pergamon Press, Oxford, 1977).
[6] R.E. Marshak, Ann. N.Y. Acad. Sci. **410**, 49 (1941).
[7] R.S. Cohen, L. Spitzer, Jr. and P. McR. Routly, Phys. Rev. **80**, 230 (1950).
[8] S.I. Braginskii, *Reviews of Plasma Physics*, M.A. Leontovich (ed.), (Consultants Bureau, New York, 1965).
[9] R.J. Hawryluk, Rev. Mod. Phys. **70**, 537 (1998).
[10] J.J. Sakurai, *Modern Quantum Mechanics*, Rev. ed., (Addison-Wesley, Reading, 1994).
[11] H. Natori and T. Munehisa, J. Phys. Soc. Jpn. **66**, 351 (1997).
[12] P.K. Chan, S. Oikawa and E. Okubo, Plasma Fusion Res. **7**, 2401034 (2012).
[13] M. Abramowitz and I.A. Stegun, *Handbook of Mathematical Functions* (Dover, 1965).